CALCULATION OF 3-D UNSTEADY SUBSONIC FLOW WITH SEPARATION BUBBLE USING SINGULARITY METHOD

Harijono Djojodihardjo[1]
Widjaja Kresna Sekar[2]
Bonifacius Prananta[3]

Center for Development of Method, Technology and Production
PT Industri Pesawat Terbang Nusantara (IPTN)
Jl.Pajajaran 154, Bandung, INDONESIA

1. ABSTRACT

A simple analytical method to calculate the unsteady airloads on an oscillating wing with separation bubbles on the suction side of the wing is presented. The oscillation of the wing is assumed to be harmonical. Linearized aerodynamics is assumed in the analysis. It is also assumed that the separation and reattachment points are known and fixed. Thus, the separation bubble does not move and the flow is separated during the whole cycle of oscillation. Such simplified model is considered beneficial for preliminary estimation of the unsteady aerodynamic characteristics of an oscillatory flow about wing with separation, such as those met in buffeting phenomenon. In order to apply the linearized potential flow theory, the flow is assumed to be inviscid and isentropic. Although such modeling is by no means a physical one, it is believed that it can serve as a mathematical convenience in obtaining the load acting in separated flow situation. Results of the method are presented. The validity of the method for fully attached flow case was insured by comparison with published results, while for separated flow cases, qualitative discussions are presented.

NOMENCLATURE

A	- source strength, doublet strength.
a_∞	- freestream velocity of sound
$a_r(y)$	- series coefficient of pressure jump.
$a_r^*(\eta)$	- normalized a_r ($a_r^* \; c(\eta)/4s$)
c	- mean chord
$c(\eta)$	- sectional chord
$C_l(\eta)$	- sectional lift coefficient
$C_L(\eta)$	- total lift coefficient
$C_m(\eta)$	- sectional moment coefficient
$C_M(\eta)$	- total moment coefficient
$\overline{C}p(\xi,\eta)$	- pressure coefficient
$\Delta\overline{C}p(\xi,\eta)$	- pressure coefficient difference ($\overline{C}p_l-\overline{C}p_u$)
$C_m(\eta)$	- sectional moment coefficient
$d_q(y)$	- series coefficient of downwash jump.
$d_q^*(\eta)$	- normalized d_q ($d_q^* \; c(\eta)/4s$)
$f_{11rs}(\xi,\eta;\eta)$, $f_{11rns}(\xi,\eta;\eta')$, $f_{12r}(\xi,\eta;\eta')$, $f_{13r}(\xi,\eta;\eta')$	- chordwise integration of the 1st Kernel function
$f_{4qs}(\xi,\eta;\eta)$, $f_{4qns}(\xi,\eta;\eta')$	- chordwise integration of the 4th Kernel function
$h_r(X)$	- pressure jump function
$h_q(X)$	- downwash jump function
$\overline{h}(X,\eta)$	- amplitude of heaving motion
i	- square root of -1
$I_1(k\|\eta-\eta'\|)$	- modified Bessel function of 1st order 1st kind
k	- $\frac{\omega s}{U_\infty}$, reduced frequency
$K_1(k\|\eta-\eta'\|)$	- modified Bessel function of 1st order 2nd kind
$K(\xi,\eta;\xi',\eta')$	- Kernel function
$L_1(k\|\eta-\eta'\|)$	- modified Struve function of 1st order
M	- Mach number
r	- $[(x-x')^2+\beta^2(y-y')^2+\beta^2(z-z')^2]^{1/2}$
s	- semi span
$(S_{rn})_{vp}$	- integration in spanwise direction of the 1st Kernel
$(S'_{qn})_{vp}$	- integration in spanwise direction of the 4th Kernel
t	- time
U_∞	- free stream velocity
$\overline{w}(\xi,\eta)$	- downwash

[1] *Vice President, Development of Methods, Technology and Production, PT IPTN and Professor, Bandung Institute of Technology*

[2] *Staff Scientist*

[3] *Staff Scientist, also Faculty Member, Bandung Institute of Technology*

$\Delta\overline{w}(\xi,\eta)$	- downwash difference $(\overline{w}_l - \overline{w}_u)$
x	- coordinate along flow direction
x_c, X_c	- pitching axis
X	- normalized coordinate in the flow direction $\left(\frac{x-x_{le}(\eta)}{c(\eta)}\right)$
y	- coordinate in spanwise direction
z	- coordinate perpendicular to xy plane
α	- amplitude of pitching oscillation
β^2	- $1-M^2$
$\phi(\xi,\eta)$	- perturbation velocity potential
$\psi(\xi,\eta)$	- acceleration potential
ω	- frequency of oscillation
η	- nondimensional y coordinate (y/s)
ξ	- nondimensional x coordinate (x/s)
τ	- $\frac{U_\infty t}{s}$, non dimensional time
μ	- M/β^2

Subscripts and Superscripts

'	- position of the singularities
D	- doublet
l	- lower surface
ns	- non singular
s	- singular
S	- source
u	- upper surface
p, j	- indices in chordwise direction
v, n	- indices in spanwise direction
le	- leading edge
te	- trailing edge
xt	- second derivative with respect to x and t
xx,yy,zz	- second derivative with respect to x,y,and z , respectively.

2. INTRODUCTION

The prediction of buffeting characteristics of aircraft remains a challenging problem for aeroelasticians. The common difficulty found by engineers in this case is usually the calculation of unsteady aerodynamic load associated with flow separation which is nonlinear in nature. For preliminary design purposes, the use of Navier Stokes solver or even the method of inviscid-viscous strong interaction to analyze the unsteady aerodynamic load may not be economically justified. In many practical applications, engineers are concerned mainly with the prediction of the load itself rather than the detail of the flow separation that occurs.

The aforementioned problem motivated many authors, such as Chi[1], Ericsson[2], Perumal[3], Dowell[4], Huber, Rocholz and Laschka[5], and Djojodihardjo, Sekar and Laschka[6] to work on this problem using a simplified model of potential flow theory. The modeling is not aimed at the physics of the flow separation itself, but rather on the load occured during the course. The results for two dimensional cases seemed to have an encouraging agreement with the experimental data. Thus, although the approaches proposed do not physically model the flow separation in great detail, they can reflect the essential mechanism present in such phenomena[6].

Since all the cases considered formerly were two dimensional, a three dimensional method would be of interest for common practical applications. This paper extends the method previously developed by Djojodihardjo et al[6] for two dimensional case and applied to wings of finite span. The kernel function method used to solve the unsteady linearized compressible potential flow without separation is extended to cover also the separated region. The boundary conditions comprise not only the slip condition on the body and no disturbance at the infinity, but also a prescribed pressure at the separated region. The three dimensional kernel function theory of Laschka[10] is adapted and modified for this case. To satisfy all the boundary conditions, doublet distribution is placed on the entire lifting surface and source distribution on the separated region.

3 PROBLEM FORMULATION

A wing modelled as a flat plate at a steady undisturbed flow having semi span equal to unity is considered. The wing is executing harmonic oscillations in pitching and heaving modes. At the upper side of the wing, separation bubbles may appear. This situation is sketched in Fig. 1.

3.1 GOVERNING EQUATION

The equation governing unsteady linearized compressible potential flow can be obtained by assuming small disturbance with respect to the free stream condition. This equation is known as the Kelvin-Bernoulli equation, which for an acceleration potential formulation reads[7]

$$(1-M^2)\psi_{xx}+\psi_{yy}+\psi_{zz}-\frac{2M}{a_\infty}\psi_{xt}-\frac{1}{a_\infty^2}\psi_{tt}=0. \quad (1)$$

For a harmonic type of oscillation this equation can further be simplified to

$$(1-M^2)\psi_{xx}+\psi_{yy}+\psi_{zz}-\frac{i2kM}{a_\infty}\psi_x+\frac{k^2}{a_\infty^2}\psi=0. \quad (2)$$

In the second equation, ψ is a complex quantity representing the amplitude of the acceleration potential and the phase lag with respect to the wing motion.

3.2 BOUNDARY CONDITIONS

a. **On the attached flow region**

The kinematical boundary condition of inviscid flow model dictates that the flow has to be tangential to the surface. This condition can be written as

$$w(x,y;\tau)=\left(\frac{\partial}{\partial x}+\frac{\partial}{\partial \tau}\right)z(x,y;\tau) \quad (3)$$

where :

$$w(x,y;\tau) = \overline{w}(x,y)e^{ik\tau} \quad (4)$$

$$z(x,y;\tau) = \overline{z}(x,y)e^{ik\tau} \quad (5)$$

and where k is the reduced frequency and τ is the nondimensional time. For a heaving and pitching motions, the surface can be represented by :

$$z(x,y;\tau) = -\overline{h}(x,y)e^{ik}, \quad (6)$$

and

$$z(x,y;\tau) = -(x-x_c)\overline{\alpha}(x,y)e^{ik\tau} \quad (7)$$

respectively. Consequently, the boundary conditions becomes,

i) for heaving motion

$$\overline{w} = -ik\overline{h} \qquad (8)$$

ii) for pitching motion

$$\overline{w} = -[1+ik(x-x_c)]\overline{\alpha}. \qquad (9)$$

b. **On the separated flow region**

The separation is considered to take place only on the upper side of the wing. On this region some assumptions have to be made regarding the velocity and the pressure of the fluid, based on the experimental evidence. The true situation may be obtained using viscous flow approach, which is beyond the scope of this work. It may be assumed that the velocity on the separated region is the same as that of the undisturbed flow. Alternatively, it may be assumed a priori that the pressure difference in the separation bubble is equal to some value γ, which may be zero [1],

$$\overline{C}p_u(x,y) = \gamma. \qquad (10)$$

4. SYSTEMS OF INTEGRAL EQUATIONS

The system of integral equation for the stated problem is obtained from two sets of integral equations. The first set is the velocity (normal wash) equation with the kinematical boundary condition on the attached region and the other is the pressure equation with the prescribed pressure boundary condition on the separated region. In each set of the integral equations, both singularities distributed on the attached and separated regions contribute to the appropriate boundary conditions. Therefore the system of integral equations comprise four components or four kernel functions. In this chapter the four kernel functions are derived.

4.1. INDUCED VELOCITY AT THE ATTACHED FLOW REGION

The first kernel of the integral equation is obtained from the induced velocity at the attached flow region. Since equation (2) is linear, then its solution for the attached flow subject to the boundary conditions can be formed by the superposition of its fundamental solution. A fundamental solution of the Kelvin Bernoulli equation for a lifting problem is the doublet flow. In the frequency domain approach of an acceleration potential formulation equation, the induced potential of a doublet point takes the form of

$$\psi_D(x,y,z) = -\frac{1}{4\pi} A e^{i\mu kM(x-x')} \frac{\partial}{\partial z}\left(\frac{e^{-i\mu kr}}{r}\right) \qquad (11)$$

where :

$$A = \frac{\Delta\overline{C}p(x',y',z')}{2}. \qquad (12)$$

The downwash at the attached flow region induced by the doublet distribution over the entire surface is then

$$\overline{w}_1(x,y) = -\frac{1}{8\pi}\int_s\int_{x_{le}}^{x_{te}} \Delta\overline{C}p(x',y')\, K_1(x,x';y,y')\, dx'dy'. \qquad (13)$$

Equation (15) is the usual integral equation of the litfing surface approach for attached flow. The kernel of this integral equation is introduced by Kussner [8] as

$$K_1 = e^{-ik(x-x')} \lim_{z\to 0} \frac{\partial}{\partial z^2} \int_{-\infty}^{x-x'} \frac{e^{ik[(x-x')/\beta^2-\mu r]}}{r}\, d(x-x') \qquad (14)$$

or in a more convenient form, as was formulated by Watkins, Runyan, Woolston [9][10] :

$$K_1 = \frac{e^{-ik(\xi-\xi')}}{s^2(\eta-\eta')^2}\Bigg\{-k|\eta-\eta'|\Bigg[K_1(k|\eta-\eta'|) + \frac{\pi i}{2}\,(I_1(k|\eta-\eta'|) - L_1(k|\eta-\eta'|)) - i - i\int_0^{U.Br} \frac{\tau}{(1+\tau^2)^{1/2}}\, e^{-ik(\eta-\eta')\tau}\, d\tau\Bigg]\Bigg\} - \frac{\xi-\xi'}{r'} e^{ik[(\xi-\xi')/\beta^2-\mu r']} \qquad (15)$$

where ξ and η are the nondimensional coordinates in x and y direction respectively, and

$$r' = [(\xi-\xi')^2+\beta^2(\eta-\eta')^2]^{1/2} \qquad (16)$$

the upper boundary of the integral is

$$U.Br = \frac{1}{|\eta-\eta'|\beta^2}\,[(\xi-\xi') - Mr'] \qquad (17)$$

4.2. INDUCED VELOCITY AT THE SEPARATED FLOW REGION

The contribution of the separated region, on which a source distribution is placed, to the first set of integral equation is derived using velocity potential formulation. Since separation occurs only in the upper surface, acceleration potential is not appropriate for this situation; velocity potential formulation is more suitable. The Kelvin - Bernoulli equation for the velocity potential formulation takes the same form as equation (2), since a linear relationship between pressure and velocity potential is assumed. The velocity potential induced by a point source is

$$\phi_S(x,y,z) = -\frac{1}{4\pi} A^+ e^{i\mu kM(x-x')}\left(\frac{e^{-i\mu kr}}{r}\right) \qquad (18)$$

At the lifting surface, a limiting process can be followed to determine the following relationship

$$\Delta\overline{w}(x',y',z') = -A^+ \qquad (19)$$

The downwash induced by the source distributed on the upper surface where the flow is separated then becomes

$$\overline{w}_1(\xi,\eta) = \int_{-1}^{1}\int_{\xi_s}^{\xi_r} \Delta\overline{w}(\xi',\eta')\; K_3(\xi,\eta;\xi',\eta')\; d\xi'd\eta' + \frac{\Delta\overline{w}}{2}\Bigg|_{\xi=\xi',\eta=\eta'} \qquad (20)$$

Notice that in the above equation the singular point has been isolated and treated separately, taking into account equation (19). The separated region for the time being is taken to be uniform in the spanwise direction; this condition can easily be modified by examining the experimental results. The kernel function of equation (20) is

$$K_3 = \frac{1}{4\pi}\lim_{z\to 0} -\beta^2 z\, \Delta\overline{w}(\xi',\eta')e^{i\mu kM(\xi-\xi')}\frac{e^{-i\mu kr'}(-i\mu kr'-1)}{r'^3} \qquad (21)$$

It is obvious that the last equation is zero on the lifting surface since linearized aerodynamics has been utilized. The remaining equation is then

$$\overline{w}_1(\xi,\eta) = \frac{\Delta\overline{w}}{2}\Big|_{\xi=\xi'\eta=\eta'} \qquad (22)$$

4.3 INDUCED PRESSURE AT THE ATTACHED FLOW REGION

The third and fourth integral equations are pressure equations, with the pressure on the upper surface where the separation occurs as the boundary condition. The third equation is obtained from the pressure induced by the doublet distribution in the the attached flow region.

From the definition of acceleration potential and the linearized Bernoulli equation the pressure coefficient is

$$\overline{C}p(x,y,z) = -2\psi_D(x,y,z). \qquad (23)$$

Taking equation (23) and equation (11) into account the pressure coefficient on the upper surface of the wing is then

$$\overline{C}p_u(\xi,\eta) = \int_{-1}^{1}\int_{\xi_{le}}^{\xi_{te}} \Delta\overline{C}p(\xi',\eta')\ K_2(\xi,\eta;\xi',\eta')\ d\xi'd\eta' - \frac{\Delta\overline{C}p}{2}\Big|_{\xi=\xi',\eta=\eta'} \qquad (24)$$

Where, again, the singularity is isolated and treated indenpendently and the separated region is distributed uniformly in the spanwise direction. The kernel function is worked out in the same manner as in two dimensional case (Djojodihardjo [6]) to obtain

$$K_2 = \frac{1}{4\pi}\lim_{z\to 0}\ \beta^2 z e^{i\mu k[M(\xi-\xi')-r']}\frac{(-i\mu kr'-1)}{r'^3} \qquad (25)$$

It can also be examined that for a planar surface, equation (26) will go to zero when z approaches zero. The remaining pressure equation then becomes a very simple equation as

$$\overline{C}p_u(\xi,\eta) = -\frac{\Delta\overline{C}p}{2}\Big|_{\xi=\xi',\eta=\eta'} \qquad (26)$$

4.4 INDUCED PRESSURE AT THE SEPARATED FLOW REGION

The kernel the last integral equation is the contribution of the velocity potential source to the pressure integral equation. The pressure coefficient is related to the velocity potential through the linearized Bernoulli equation as

$$\overline{C}p(x,y,z) = -2\left(\frac{\partial\phi_s}{\partial\tau} + \frac{\partial\phi_s}{\partial x}\right) \qquad (27)$$

Substituting the expression of induced velocity potential due to sources distributed on the separated region into equation (27), one obtains the pressure at the upper surface in the form

$$\overline{C}p_u(\xi,\eta) = \int_{-1}^{1}\int_{\xi_s}^{\xi_r} \Delta\overline{w}(\xi',\eta')\ K_4(\xi,\eta;\xi',\eta')\ d\xi'd\eta' \qquad (28)$$

where, the kernel

$$K_4 = -\frac{1}{2\pi}e^{i\mu k[M(\xi-\xi')-r']}\left(\frac{ik}{\beta^2 r'} - \frac{(\xi-\xi')(i\mu k+1/r')}{r'^2}\right) \qquad (29)$$

Superposing all the components contributing to the integral equation as elaborated in this section, the system of integral equation is found to be

$$\overline{w}_1(\xi,\eta) = \int_{-1}^{1}\int_{\xi_{le}}^{\xi_{te}} \Delta\overline{C}p(\xi',\eta')\ K_1(\xi,\eta;\xi',\eta')\ d\xi'd\eta' + \frac{\Delta\overline{w}}{2}\Big|_{\xi=\xi',\eta=\eta'} \qquad (30)$$

$$\overline{C}p_u(\xi,\eta) = \int_{-1}^{1}\int_{\xi_s}^{\xi_r} \Delta\overline{w}(\xi',\eta')\ K_4(\xi,\eta;\xi',\eta')\ d\xi'd\eta' - \frac{\Delta\overline{C}p}{2}\Big|_{\xi=\xi',\eta=\eta'} \qquad (31)$$

This system of integral equation comprises two Fredholm integral equations of the second kind, since the unknowns also exist outside the integrals.

5 METHOD OF SOLUTION

As has been mentioned in the beginning of this paper, the method employed for solving the system of integral equation is the so called kernel function method. The solution is assumed to stem in a function space which must satisfy the physical characteristics of the solution. Each component of the function space is valid throughout the domain (in this case the lifting surface); this is the main difference as compared to the finite element approach where the function space is only valid in an element. The choice of the series of functions is carried out taking into consideration four aspects, namely the completeness of the function space, the physical characteristic modelled, the convenience of the integration, and the rapid convergence of the series.

In the present work, the unknowns, the distributions of pressure difference and downwash jump across the lifting surface are represented by the series expansion as

$$\Delta\overline{C}p(X,y) = \sum_{r=0}^{R} a_r(y)\ h_r(X) \qquad (32)$$

in which each function $h_r(X)$ should exhibit a well known singularity behavior for $X \to 0$ of the type,

$$\lim_{\varepsilon\to 0}\ \varepsilon^{-1/2}$$

This singularity models the suction force at the leading edge. At the trailing edge where Kutta condition applies, the result of thin airfoil theory dictates that the pressure difference should go to zero in a manner like

$$\lim_{\varepsilon\to 0}\ \varepsilon^{1/2}$$

One set of functions which satisfies those physical characteristics in the chordwise direction is the one introduced by Glauert [10]

$$h_r(X) = \frac{2}{\pi}\,\frac{\cos(r\phi)+\cos((r+1)\phi)}{\sin\phi} \qquad (33)$$

where

$$X = \frac{x-x_{LE}(\eta')}{c(\eta')} = \frac{1}{2}(1-\cos\phi) \qquad (34)$$

The collocation points are defined as

$$\phi = \frac{2\pi(p+1)}{2P+3}, \quad p = 0,1,\ldots,P \tag{35}$$

The coefficients of the series are not constants, but they will also be expanded in the spanwise direction, taking into account the physical characteristics of the flow.

Similarly for the downwash jump across the lifting surface, the same series expansion is used

$$\Delta\overline{w}(X,y) = \sum_{q=0}^{Q} d_q(y)\ h_q(X) \tag{36}$$

After substitution of the series expansion, the system of integral equations becomes

$$\overline{w}_l(\xi,\eta) = \sum_{r=0}^{R} \int_{-1}^{1} a_r^*(\eta') \int_{\xi_{le}}^{\xi_{te}} h_r(X)\ K_1(\xi,\eta;\xi',\eta')\ d\xi' d\eta'$$

$$+ \sum_{q=0}^{Q} \int_{-1}^{1} d_q^*(\eta') \left.\frac{h_q(X)}{2}\right|_{\xi=\xi',\eta=\eta'} d\eta' \tag{37}$$

$$\overline{C}p_u(\xi,\eta) = \sum_{q=0}^{Q} \int_{-1}^{1} d_q^*(\eta') \int_{\xi_s}^{\xi_r} h_q(X)\ K_4(\xi,\eta;\xi',\eta')\ d\xi' d\eta'$$

$$+ \sum_{r=0}^{R} \int_{-1}^{1} a_r^*(\eta') \left.\frac{h_r(X)}{2}\right|_{\xi=\xi',\eta=\eta'} d\eta' \tag{38}$$

The asterisks in the coefficients stand for the apropriate nondimensionalization of the coefficients in the spanwise direction. After the integration in the chordwise direction, the above set of equations can be written as

$$\overline{w}_l(\xi,\eta) = \sum_{r=0}^{R} \int_{-1}^{1} a_r^*(\eta')\ f_{1r}(\xi,\eta;\eta')\ d\eta' +$$

$$\sum_{q=0}^{Q} \int_{-1}^{1} d_q^*(\eta') \left.\frac{h_q(X)}{2}\right|_{\xi=\xi',\eta=\eta'} d\eta' \tag{39}$$

$$\overline{C}p_u(\xi,\eta) = \sum_{r=0}^{R} \int_{-1}^{1} a_r^*(\eta') \left.\frac{h_r(X)}{2}\right|_{\xi=\xi',\eta=\eta'} d\eta' +$$

$$\sum_{q=0}^{Q} \int_{-1}^{1} d_q^*(\eta')\ f_{4q}(\xi,\eta;\eta')\ d\eta' \tag{40}$$

The charateristic of the flow in the spanwise directions can be well represented by expanding the coefficients $a_r^*(\eta)$ and $d_q^*(\eta)$ in a Fourier sine series. Introducing a coordinate transformation, where $\eta = \cos(\theta)$, the series can be written as

$$a_r^*(\theta) = \sum_{\mu=1}^{M} A_\mu \sin(\mu\theta) \tag{41}$$

The integration in the spanwise direction is worked out using Multhopp method, which is closely related to the choice of the series. Subtituting the series into the system of integral equation and carrying out the integration, one obtains

$$\overline{w}_l(\xi,\eta) = \sum_{r=0}^{R} \sum_{m=1}^{M} a_{rm}^* c1_{rm} f_{1r}(\xi,\eta;\theta_m) + \sum_{q=0}^{Q} \sum_{m=1}^{M} d_{qm}^* c2_{rm} \frac{h_{qm}}{2}$$

$$\overline{C}p_u(\xi,\eta) = \sum_{r=0}^{R} \sum_{m=1}^{M} a_{rm}^* c3_{rm} \frac{h_{rm}}{2} + \sum_{q=0}^{Q} \sum_{m=1}^{M} d_{qm}^* c4_{rm} f_{4q}(\xi,\eta;\theta_m)$$

c1, c2, c3, c4 are the quadrature constants of the Multhopp integration method.

The last set of equations indicates the presence of M(R+1) number of unknowns, in the form of coefficients of expansions. The same number of collocation points, where the equation has to be satisfied, should be taken. The collocation points in the chordwise direction has been introduced before, namely

$$\phi = \frac{2\pi(p+1)}{2P+3}, \quad p = 0,1,\ldots,P \tag{35}$$

In the spanwise direction the collocation points are chosen to follow a cosine spacing

$$\theta = \frac{v\pi}{V+1}, \quad v = 1,2\ldots,V \tag{44}$$

To have the same number of collocation points P must be equal to R and V must be equal to M. The set of algebraic equations at the collocation points are

$$\overline{w}_{l\ pv} = \sum_{r=0}^{R} \sum_{m=1}^{M} a_{rm}^* g_{1\ rm\ pv} + \sum_{q=0}^{Q} \sum_{m=1}^{M} d_{qm}^* g_{3\ qm\ pv} \tag{45}$$

$$\overline{C}p_{u\ pv} = \sum_{r=0}^{R} \sum_{m=1}^{M} a_{rm}^* g_{2\ rm\ pv} + \sum_{q=0}^{Q} \sum_{m=1}^{M} d_{qm}^* g_{4\ rm\ pv} \tag{46}$$

where p and v run from 0 to P and from 1 to V respectively. The equation in the matrix form

$$\begin{bmatrix} g_1 & g_3 \\ g_2 & g_4 \end{bmatrix} \begin{Bmatrix} a^* \\ d^* \end{Bmatrix} = \begin{Bmatrix} \overline{w}_l \\ \overline{C}p_u \end{Bmatrix}. \tag{47}$$

Solving this set of algebraic equations, the coefficients of the series expansion are obtained.

The pressure coefficient and the other aerodynamic coefficients can then be easily calculated from this result.

6. PRESSURE, LIFT & MOMENT COEFFICIENT

The pressure coefficient consists of the attached and separated part, which are calculated separately. Both of them give their contribution to the lift and moment coefficients.

$$\Delta\overline{C}p(X,\eta) = \begin{cases} \Delta\overline{C}p_{att}(X,\eta) & \text{for } 0<x<x_s \text{ and } x_r<x<c(\eta) \\ \Delta\overline{C}p_{sep}(X,\eta) & \text{for } x_s<x<x_r \end{cases}$$

The pressure difference on the attached region can directly be calculated from the series expansion as,

$$\Delta\overline{C}p_{att}(X,\eta) = \sum_{r=0}^{R} a_r(\eta)^* h_r(X) \tag{76}$$

The pressure difference at the separated region may be calculated using the following procedure. The definition of pressure difference is

$$\Delta\overline{C}p_{sep}(X,\eta) = \overline{C}p_l(X,\eta) - \overline{C}p_u(X,\eta) \tag{77}$$

The lower pressure coefficient is calculated simply from

$$\overline{C}p_l(X,\eta) = \sum_{r=0}^{R} a_r(\eta) \frac{h_r(X)}{2} \tag{78}$$

and from the pressure integral equation, the upper pressure is

$$\overline{C}p_u(X,\eta) = -\sum_{r=0}^{R} a_r(\eta) \frac{h_r(X)}{2} + \sum_{q=0}^{Q} \sum_{m=1}^{M} d_{qm}\ g_{4\ qm\ vp} \tag{79}$$

Substituting the two expressions of the upper and lower pressure, the pressure difference is then

$$\Delta\overline{C}p(X,\eta) = \sum_{r=0}^{R} a_r(\eta)^* h_r(X) - \sum_{q=0}^{Q} \sum_{m=1}^{M} d_{qm} g_{4qmvp} \tag{80}$$

The sectional lift coefficient may then be calculated as

$$C_l(\eta)=\int_0^{X_s} \bar{\Delta}Cp_{att}(X',\eta)\ dX'+\int_{X_s}^{X_r} \Delta\bar{C}p_{sep}(X',\eta)\ dX'$$

$$= a_0(\eta) - \sum_{q=0}^{Q} \sum_{m=1}^{M} d_{qm} \sum_{J=0}^{J} g_{1\ qm\ vp} \sin\phi_J \left(\frac{\phi_r-\phi_s}{2(J+1)}\right) \quad (81)$$

The sectional moment coefficient is calcualated in the same manner as the lift coefficients

$$C_m(\eta)=-\int_0^{X_s} \bar{\Delta}Cp_{att}(X',\eta)(X'-X_c)dX'$$

$$-\int_{X_s}^{X_r} \Delta\bar{C}p_{sep}(X',\eta)(X'-X_c)dX'$$

$$= \frac{1}{4}\ [a_1(\eta)+(4X_c-1)a_0(\eta)] +$$

$$\sum_{q=0}^{Q} \sum_{m=1}^{M} d_{qm} \sum_{J=0}^{J} g_{4\ qm\ vp}(X_J-X_c)\sin\phi_J \left(\frac{\phi_r-\phi_s}{2(J+1)}\right) \quad (82)$$

The wing lift coefficient is obtained by integrating the sectional lift coefficient in the spanwise direction

$$C_L= \frac{1}{S} \int_{-s}^{s} C_l(y)c(y)\ dy$$

$$= \frac{\pi}{S\bar{M}} \sum_{m=1}^{M} C_l(\theta_m)c(\theta_m)\sin\theta_m \quad (83)$$

In the same manner the momment coefficient of the wing is

$$C_M = \frac{1}{Sc} \int_{-s}^{s} C_m(y)c^2(y)\ dy$$

$$= \frac{\pi}{S\bar{c}M} \sum_{m=1}^{M} C_m(\theta_m)c^2(\theta_m)\sin\theta_m \quad (84)$$

7. RESULTS

Figures 2a and 2b show the sectional lift and moment coefficients, respectively, for pitching oscillations pivoted at Xc = 0.5 in a fully attached flow, for a lifting surface with an aspect ratio of 2, and for incompressible case. For Mach number of 0.8, the results are shown by Figs. 3a and 3b. The results agree very well with those obtained by Laschka. Similarly, for heaving oscillations, the results are exhibited in Figs 4a and 4b for incompressible case and Figs. 5a and 5b for Mach number of 0.8. Both oscillation were calculated at a reduced frequency of 1.00. The moment coefficients of the pitching oscillation have been referred to the pivot point, while for heaving oscillation to the quarter chord. The agreement appears to be very good. The slight difference indicated in the results may be attributed to numerical errors in approximating the integral, since this difference behaves consistently. The distribution of pressure differences in the chordwise direction is presented in Figs. 6a and 6b. These are the case of pitching oscillations around mid chord with reduced frequency of 2 for a wing with aspect ratio of 2 in incompressible flow. Again the results exhibit good agreement with those of Laschka's.

For the separated three dimensional flow case to the best of the author's knowledge no theoretical results, under the similar assumptions, as well as experimental results, for a fixed separation point, are available. Therefore we would like to embark upon a qualitative comparisons to existing data. As a first step towards this end, computational results for steady state case at Mach number 0.147 for a wing with separation point at 35% chord and for fully separated wing are shown in Figs. 7b and 7c, while the fully attached flow case is shown in Fig. 7a. These results are compared to experimental ones obtained at IPTN, both for a wing with aspect ratio of 4.4. However since for the experimental case finite thickness wing was employed and our mathematical model does not take thickness effects into account, the comparison can only be interpreted qualitatively. Taking these into considerations, we could conclude that satisfactory qualitative agreement between our work and experimental data has been exhibited.

Figures 8a and 8b show the real and imaginary sectional moment coefficients of the wing having aspect ratio 2 executing an oscillatory motion in pitching mode, pivoted at half chord. Two reduced frequencies were calculated to see its effect on moment coefficients. This is the case of incompressible with partially separated flow on the upper side; the separation is started at 60% chord. The results of the present method are compared to the three dimensional ones of the strip theory corrected with elliptic downwash of Ref. [12]. The two dimensional theory used in the strip theory is the one developed by the authors[6]. The differences exhibited in Figs. 8a and 8b have been expected to appear, since the strip theory uses a simple prescribed downwash. Consistent differences shown between the two results indicate correct tendencies as the reduced frequency increases.

The effect of separation is shown in Figs. 9a through 9b for the same Mach number and vibration mode as the previous case. Two cases were calculated namely fully attached and separated flow starting from 60% chord. The results again are compared to the strip theory with prescribed elliptic downwash. Both methods show a decrease in lift coefficients due to separation as expected. Conclusion similar to that of Figs. 8a and 8b can be drawn for Figs. 9a and 9b.

8. CONCLUSION

Extension of the linearized theory for unsteady two dimensional subsonic flow around oscillating airfoil with separated region has been carried out for finite wings. Although comparison with the results of other three dimensional theoretical work can not be made due to lack of data, comparison with strip theory based on two dimensional results corrected with a simple prescribed downwash, shows a correct tendency.

9. FURTHER RESEARCH

The approach taken here is linearized aerodynamics, and planar surface has been implicitly treated throughout. However, for non-planar surfaces, the work can be extended by approximating the surface by finite set of planar elements and by the use of modified series expansion taking into account the local angle of incidence. The kernel functions can then be evaluated numerically or exactly, wherever appropriate, similar to the procedure adopted here. Another alternative is to utilize doublet lattice approach. This will be the subject of future work. The applicability of the present work to flutter and buffeting problems should next be investigated.

10. REFERENCES

[1] Chi, R.M., *Separated Flow Unsteady Aerodynamic Theory* , J. Aircraft Vol. 22, No. 11 , 1985

[2] Ericsson, L.E. and Reding, J.P., *Unsteady airfoil stall, Review and Extention*, AIAA Journal vol. 8, August 1981, pp 609-616.

[3] Perumal, P.V.K. and Sisto, F., *Lift and Moment Prediction for an Oscillating Airfoil with Moving Separation Point*, ASME Transaction, Journal of Engineering of Power, Vol. 96, October 1974, pp 372-378.

[4] Dowell, E.H., *A Simplified Theory of Oscillating Airfoil in Transonic Flow: Review and Extention*, AIAA Paper 77-445, March 1977.

[5] Huber, Th., Rochholz, B., Laschka , B., *Modelling of Separated Flow Around Oscillating Cascade by Classical Singularity Method*, International Forum on Aeroelasticity and Structural Dynamics, Aachen, June 3-6, 1991.

[6] Djojodihardjo, H., Sekar, W.K., Laschka, B., *Calculation of Pressure Distribution on Two-Dimensional Wing in Unsteady Subsonic Flow with Separation Bubble using Kernel Function Method*, International Forum on Aeroelasticity & Structural Dynamics, Aachen, FR Germany, 1991.

[7] Bisplinghoff, R.L., Ashley, H. and Halfman, *Aeroelasticity*, Addison Wesley, Reading, Massachussets, 1955

[8] Kuessner, H.G., *Allgemeine Tragflachentheorie*, Luftfahrtforschung No. 17, 1940, pp 370-378.

[9] Watkins, C.E., Runyan, H.L., Woolston, D.S., *On the Kernel Function of the Integral Equations relating the Lift and Downwash Distributions of Oscillating Finite Wing in Subsonic Flow*, NACA Rep.1234, 1955.

[10] Laschka, B., *Zur Theorie der Harmonisch-schwingenden,Tragenden Flaeche bei Unter-schallanstroemung*, Zeitschrift fuer Flugwissen schaften, Braunschweig, 1963.

[11] Watkins, C.E., Woolston D.S. and Cunningham H.J., *A Systematic Kernel Function Procedures for Determining Aerodynamics Forces on Oscillating or Steady Finite Wing at Subsonic Speed*, NASA TR R-48, 1960.

[12] Djojodihardjo, H., Sekar, W.K., *Calculation of Unsteady Aerodynamic Load on a Finite Span Wing with Separated Region using Strip Theory Approach,* IPTN Internal Report, 1991.

APPENDIX A THE SINGULAR PART OF KERNEL FUNCTIONS

Noting the complexity of the kernel functions, it is intended to integrate them using numerical approach. It is obvious that the singularity contained in the kernel functions will tend to spoil the numerical integration if they are not carefully treated. The usual technique to take care of this problem is to isolate the region in the vicinity of the singular point, and to integrate it in an analytical manner applying a suitable limitting process. The remaining regular kernel can then be easily and accurately integrated using a standard numerical quadrature. The limitting processes for the second and third kernel are well documented in many literatures. Such procedure leads to equation (30) and (31). Hereafter, the singularities of the first and fourth kernel are presented.

The integral in the chordwise direction will contain singularities if η and η' take the same values. This situation is closely related to the integration technique applied for the spanwise direction. The singular part of the first kernel can be examined to consist of some poles and a logarithmic function, since the Bessel function has a logarithmic behaviour for small arguments. This singular part is [10]

$$K_{1s}(\xi,\eta;\xi',\eta') = \frac{e^{-ik(\xi-\xi')}}{s^2}\left[-\frac{1}{(\eta-\eta')^2}\left|1+\frac{\xi-\xi}{r'}\right| + \frac{ik}{r'} - \frac{k^2}{2}\ln\,[r'-(\xi-\xi')]\right] \quad \text{(A.1)}$$

The singular part of the fourth kernel has a less complexity since the singularity is caused only by the r'. Consequently it produces some poles, which can be taken separately as

$$K_{4s}(\xi,\eta;\xi',\eta') = -\frac{1}{2\pi}\left[\frac{ik}{\beta^2|\xi-\xi'|}\left(1-\frac{M(\xi-\xi')}{|\xi-\xi'|}\right) - \frac{(\xi-\xi')}{|\xi-\xi'|^3}\right] \quad \text{(A.2)}$$

If these two singular parts obtained are subtracted from the original kernels, the rest will become regular functions which facilitate the numerical treatment of them. Proceeding along this line, then the non singular of the first and fourth kernel are

$$K_{1ns}(\xi,\eta;\xi',\eta') = K_1(\xi,\eta;\xi',\eta') - K_{1s}(\xi,\eta;\xi',\eta') \quad \text{(A.3)}$$

and

$$K_{4ns}(\xi,\eta;\xi',\eta') = K_4(\xi,\eta;\xi',\eta') - K_{4s}(\xi,\eta;\xi',\eta'). \quad \text{(A.4)}$$

APPENDIX B INTEGRATION IN CHORDWISE DIRECTION

The integration of the first kernel is worked out exactly in the same manner as the one in Laschka [10], where the singular parts are treated analytically and the rest numerically. Proceeding along Laschka's approach the singular integral is divided into three parts

$$f_{1r}(\xi,\eta;\eta) = -\frac{1}{2\pi}\sum_{r=0}^{R}\left\{\lim_{\varepsilon\to 0}\left[\frac{2}{\varepsilon}a_r^*(\eta)\,f_{11rs}(\xi,\eta;\eta) - \int_{-1}^{1}\frac{a_r^*(\eta')}{(\eta-\eta')}f_{11rns}(\xi,\eta;\eta')\,d\eta'\right] + \int_{-1}^{1}a_r^*(\eta')\,\ln|\eta-\eta'|\;f_{12r}(\xi,\eta;\eta')\,d\eta' + \int_{-1}^{1}a_r^*(\eta')\,f_{13r}(\xi,\eta;\eta')\,d\eta'\right\} \quad \text{(B.1)}$$

The Gauss-Jacobian Quadrature is employed for the integration of the nonsingular kernel times the series expansion. The quadrature chosen takes the advantage of the series expansion, h_r (X), as the weighting function,

$$L(r,X) = \int_0^1 h_r(X')\;F(X,\eta;X',\eta')\;dX' = \sum_{J=0}^{J} B_{rJ}\;F(X,\eta;X_J,\eta') \quad \text{(B.2)}$$

where :

$$B_{rJ} = \frac{\cos(r\phi_J)+\cos((r+1)\phi_J)}{J+1} \quad \text{(B.3)}$$

The components of f_{1r} $(\xi,\eta;\eta)$is then evaluated one by one using this formula as

$$f_{11rs}(\xi,\eta;\eta) = \sum_{j=0}^{J} B_{rj}\,e^{-ik\frac{c(\eta)}{s}(X-X_j)}\left(1+\frac{X-X_j}{R_j}\right) \quad \text{(B.4)}$$

$$f_{11rns}(\xi,\eta;\eta') = f_{1rs}(\xi,\eta;\eta') + \left(\frac{dh_r(X)}{dX'} + ik\,\frac{c(\eta)}{s} h_r(X)\right) \left(\frac{\beta s}{c(\eta)}\right)^2 (\eta-\eta')^2 \ln|\eta-\eta'| \tag{B.5}$$

$$f_{12r}(\xi,\eta;\eta') = -k^2 \sum_{j=0}^{J} B_{rj} e^{-ik\frac{c(\eta)}{s}(X-X_j)} + \left(\frac{\beta s}{c(\eta)}\right)^2 \left[\frac{dh_r(X)}{dX'} + ik\,\frac{c(\eta)}{s} h_r(X)\right] - 2ik\,\frac{s}{c(\eta')} h_r(X) \tag{B.6}$$

$$f_{13r}(\xi,\eta;\eta') = \frac{f_{1rns}(\xi,\eta;\eta')}{(\eta-\eta')^2} - \ln|\eta-\eta'|\; f_{2r}(\xi,\eta;\eta') - \frac{1}{(\eta-\eta')^2}\sum_{j=0}^{J} B_{rj}\, e^{-ik\frac{c(\eta)}{s}(X-X_j)} \Bigg\{ k|\eta-\eta'| \Bigg[K_1(k|\eta-\eta'|) - i + \frac{\pi i}{2}\left(I_1(k|\eta-\eta'|) - L_1(k|\eta-\eta'|)\right) - i\int_0^{U.Br} \frac{\tau}{(1+\tau^2)^{1/2}}\, e^{-ik(\eta-\eta')\tau}\, d\tau\Bigg] + \frac{X-X_j}{R}\, e^{-ik\frac{c(\eta)}{s\beta^2}(X-X_j-MR_j)} \Bigg\} \tag{B.7}$$

where the upper boundary of the integral becomes

$$U.Br = \frac{(X-X'-MR)}{\beta^2|\eta-\eta'|}\,\frac{c(\eta')}{s} \tag{B.8a}$$

and

$$R = \left[(X-X')^2 + \beta^2\frac{s^2}{c^2(\eta')}(\eta-\eta')^2\right]^{\frac{1}{2}} \tag{B.8b}$$

$$X' = \frac{x' - x_{LE}(\eta')}{c(\eta')} = \frac{1}{2}(1-\cos\phi') \tag{B.8c}$$

$$\phi' = \frac{j\pi}{J+1} \tag{B.8d}$$

$$j = 0,1,\ldots,J \tag{B.8e}$$

Following Watkins et.al[11], the approximation of the integrand is carried out by expansion like,

$$\frac{\tau}{(1+\tau^2)^{1/2}} \cong 1 - 0.101\, e^{-0.329\tau} - 0.899\, e^{-1.4067\tau} - 0.09480933 e^{-2.90\tau} \sin \pi\tau \tag{B.9}$$

Using this expression the integral appeared in equation (B.7) can be easily worked out to obtain,

$$\int_0^{U.Br} \frac{\tau}{(1+\tau^2)^{1/2}} e^{ik(\eta-\eta')\tau}\, d\tau = \frac{e^{ik|\eta-\eta'|U.Br} - 1}{ik|\eta-\eta'|} - \frac{0.101(e^{(ik|\eta-\eta'|-0.329)U.Br}-1)}{ik|\eta-\eta'|-0.329} - \frac{0.899(e^{(ik|\eta-\eta'|-1.4067)U.Br}-1)}{ik|\eta-\eta'|-1.4067} - 0.09480933\, C$$

with:

$$C = \frac{\dfrac{-(e^{(ik|\eta-\eta'|-2.90)U.Br}\cos(\pi U.Br)-1)}{\pi}}{\left[1+\dfrac{1}{\pi^2(ik|\eta-\eta'|-2.90)^2}\right]} + \frac{\dfrac{e^{(ik|\eta-\eta'|-2.90)U.Br}\sin(\pi U.Br)}{\pi^2(ik|\eta-\eta'|-2.90)}}{\left[1+\dfrac{1}{\pi^2(ik|\eta-\eta'|-2.90)^2}\right]} \tag{B.11}$$

An efficient approximation to the Bessel and Struve functions that appear in the equation (B.7) are [11]

$$I_1(k|\eta-\eta'|) - L_1(k|\eta-\eta'|) \cong \frac{2k|\eta-\eta'|}{\pi} \left\{ \frac{1.0085\, k|\eta-\eta'|}{1.3410 + 1.0050k^2(\eta-\eta')^2} + \left[\frac{\pi}{4} - 0.8675k|\eta-\eta'|\left(\frac{0.4648+0.9159k|\eta-\eta'|}{1.3410+k^2(\eta-\eta')^2}\right)\right] e^{-k|\eta-\eta'|} \right\}$$

In the same manner, the integration in the chordwise direction for the fourth kernel reads

$$f_{4qns}(\xi,\eta;\eta') = -\sum_{j=0}^{J} B_{qj}\Bigg[\frac{e^{i\mu k[M(X-X_j)-R_j]s/c(\eta')}}{2\pi}\left\{\frac{ik}{\beta^2 R_j} - \frac{(X-X_j)\; i\mu k}{R_j^2} - \frac{s}{c(\eta')}\,\frac{(X-X_j)}{R_j^3}\right\} - \left\{-\frac{1}{2\pi}\left\{\frac{ik}{\beta^2|X-X_j|}\left(1-\frac{M(X-X_j)}{|X-X_j|}\right) - \frac{s}{c(\eta)}\,\frac{(X-X_j)}{(X-X_j)^3}\right\}\right\}\Bigg]\frac{\phi_r-\phi_s}{\pi}$$

for $X > X_j$:

$$f_{4qs}(\xi,\eta;\eta) = \sum_{j=0}^{J} \frac{-ik}{2\pi^2\beta^2}(1-M)(I1_q + I1_{q+1}) + \frac{1}{2\pi^2}(I2_q + I2_{q+1})$$

for $X < X_j$:

$$f_{4qs}(\xi,\eta;\eta) = \sum_{j=0}^{J} \frac{ik}{2\pi^2\beta^2}(1+M)(I1_q + I1_{q+1}) - \frac{1}{2\pi^2}(I2_q + I2_{q+1}) \tag{B.12}$$

with :

$$I1_q = \frac{1}{2\sin\phi}\left[\cos(q\phi)\bar{J}_q + \sin(q\phi)\bar{K}_q\right]$$

$$I2_q = \frac{1}{4\sin^2\phi}\Big\{\cos(q\phi)\bar{L}_q + \sin(q\phi)\bar{M}_q + \cot(\phi)[\cos(q\phi)\bar{J}_q + \sin(q\phi)\bar{K}_q] + \frac{1}{2\sin\phi}[\cos(m\phi)\bar{J}_m + \sin(m\phi)\bar{K}_m + \cos(k\phi)\bar{J}_k + \sin(k\phi)\bar{K}_k]\Big\} \tag{B.13}$$

with : $m = q + 1$ and $k = q - 1$

For $q = 0$:

$$\bar{J}_q = 2\ln\left|\frac{\sin\left(\frac{\phi+\phi_r}{2}\right)\sin\left(\frac{\phi-\phi_r}{2}\right)}{\sin\left(\frac{\phi+\phi_s}{2}\right)\sin\left(\frac{\phi-\phi_s}{2}\right)}\right| , \quad \bar{K}_q = 0$$

$$\bar{L}_q = -2\left[\cot\left(\frac{\phi+\phi_r}{2}\right) - \cot\left(\frac{\phi+\phi_s}{2}\right) - \cot\left(\frac{\phi-\phi_r}{2}\right) + \cot\left(\frac{\phi-\phi_s}{2}\right)\right] - 2(\phi_r-\phi_s) , \quad \bar{M}_q = 0 \tag{B.14}$$

For $q = 1$:

$$\bar{J}_q = \bar{J}_{q-1} + 2\sin\phi(\sin\phi_s - \sin\phi_r) , \quad \bar{L}_q = \bar{L}_{q-1} - \bar{K}_q$$

$$\bar{K}_q = 2(\phi_r-\phi_s) + 2\cos\phi(\sin\phi_r - \sin\phi_s) , \quad \bar{M}_q = \bar{M}_{q-1} + \bar{J}_q + \bar{J}_{q-1} \tag{B.15}$$

For $q > 1$:

$$\bar{J}_q = \bar{J}_{q-1} + \frac{2}{q-1}\sin(q-1)\phi[\sin(q-1)\phi_s - \sin(q-1)\phi_r]$$

$$+ \frac{2}{q}\sin(q\phi)[\sin(q\phi_s) - \sin(q\phi_r)] , \qquad \bar{L}_q = \bar{L}_{q-1} - \bar{K}_{q-1} - \bar{K}_q$$

$$\bar{K}_q = \bar{K}_{q-1} + \frac{2}{q-1}\cos(q-1)\phi[\sin(q-1)\phi_r - \sin(q-1)\phi_s]$$

$$+ \frac{2}{q}\cos(q\phi)[\sin(q\phi_r) - \sin(q\phi_s)] , \qquad \bar{M}_q = \bar{M}_{q-1} + \bar{J}_q + \bar{J}_{q-1} \qquad \text{(B.16)}$$

APPENDIX C INTEGRATION IN SPANWISE DIRECTION

In the spanwise direction the integation is performed in a similar way as in steady case where Multhopp's method is employed. The method is based on the assumption that the characteristics of the flow in the spanwise direction can be excellently approximated by a Fourier sine series. The coefficient of expansion as a function of η can then be written as

$$a_r^*(\theta) = \sum_{\mu=1}^{M} A_\mu \sin(\mu\theta) \qquad \text{(C.1)}$$

using the coordinate transformation where $\eta = \cos(\theta)$ The series coeffcient can be calculated by the orthogonality of the series

$$\int_0^\pi \sum_{\mu=1}^{M} A_\mu \sin(\mu\theta)\sin(m\theta)\,d\theta = \int_0^\pi a_r^*(\theta)\sin(m\theta)\,d\theta$$

Applying Multhopp integration quadrature for the right hand side results

$$A_\mu = \frac{2}{M+1}\sum_{m=1}^{M}\sin(\mu\theta_m)\,a_r^*(\theta_m) \qquad \text{(C.2)}$$

The integration points are also the collocation points in the spanwise direction, namely

$$\theta_m = \frac{m\pi}{M+1} \quad \text{with} \quad m=1,2,\ldots,M \qquad \text{(C.3)}$$

The same integration technique is applied to the integration of the kernel function in the spanwise direction. Notice that the downwash has to be evaluated at the collocation points

$$\bar{w}_{l\,pv} = \sum_{r=0}^{R}\sum_{m=1}^{M} a_{rm}^*\, cl_{rm}\, f_{lrm\,pv} \qquad \text{(C.4)}$$

The kernel function is divided into three parts, i.e.:

$$cl_{rm} f_{lrm} = b_{rm}(f_{11rm})_{pv} + c_{rm}(f_{12rm}\,\sigma_n\, f_{13rm})_{vp} \qquad \text{(C.5)}$$

$$b_{vm} = \begin{cases} -\dfrac{1-(-1)^{v-m}}{2(M+1)}\dfrac{\sin\theta_m}{(\cos\theta_v - \cos\theta_m)^2} & \text{for } v \neq n \\ \dfrac{M+1}{4\sin\theta_v} & \text{for } v = n \end{cases} \qquad \text{(C.6)}$$

$$\sigma_m = \frac{\sin\theta_m}{2(M+1)} \qquad \text{(C.7)}$$

$$c_{vm} = \frac{1}{2(M+1)}\left\{\sin\theta_m\left[\frac{1}{2}\cos 2\theta_v - \ln 2\right] + \sum_{\mu=2}^{M}\sin(\mu\theta_m)\left[\frac{\cos(\mu+1)\theta_v}{\mu+1} - \frac{\cos(\mu-1)\theta_v}{\mu-1}\right]\right\} \qquad \text{(C.8)}$$

where f_{11rm}, f_{12rm} and f_{13rm} are given by equations (B.4), (B.5), (B.6), and (b.7). The same quadrature is applied to the integration of the fourth kernel.

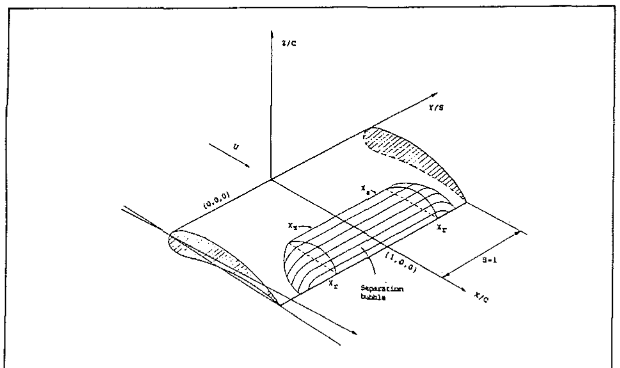

Fig. 1a. Schematic of a Wing with Separation bubble
Ideal situation

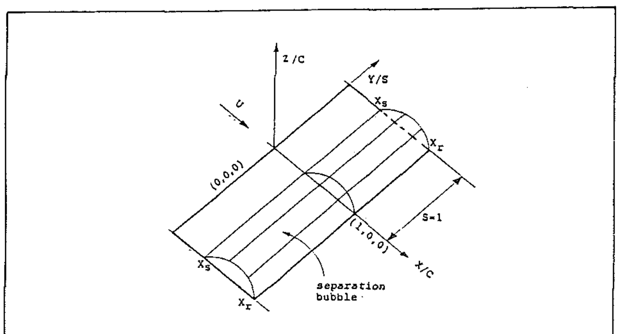

Fig. 1b. Schematic of a Wing with Separation bubble
Linearized situation
Xs & Xr assumed constant along spanwise
Xr assumed at Xte

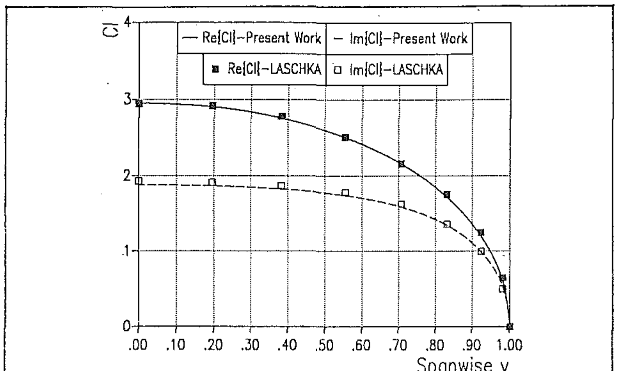

Fig. 2a. Sectional Lift Coefficient
Case : Fully Attached Flow, Pitching motion
M = 0.0, Xc = 0.5, k = 1.0, AR = 2

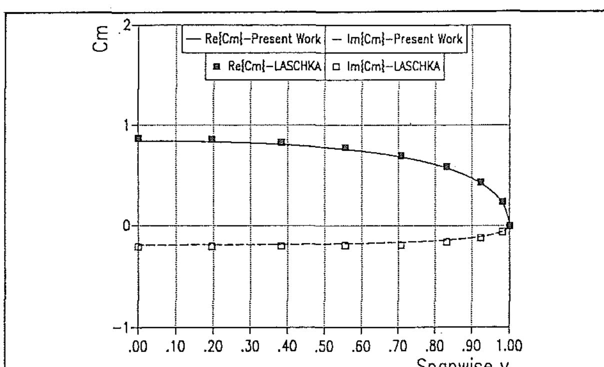

Fig. 2b. Sectional Moment Coefficient
Case : Fully Attached Flow, Pitching motion
M = 0.0, Xc = 0.5, k = 1.0, AR = 2

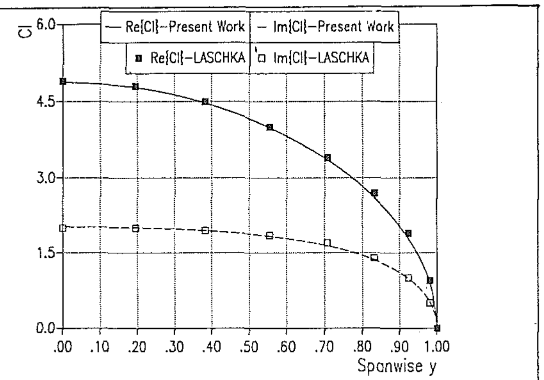

Fig. 3a. Sectional Lift Coefficient
Case : Fully Attached Flow, Pitching Motion
M = 0.8, Xc = 0.5, k = 1.0, AR = 2

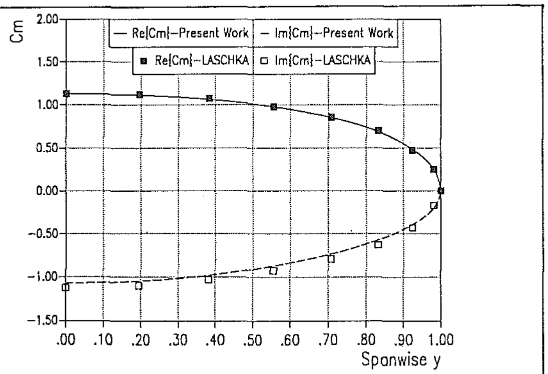

Fig. 3b. Sectional Moment Coefficient
Case : Fully Attached Flow, Pitching Motion
M = 0.8, Xc = 0.5, k = 1.0, AR = 2

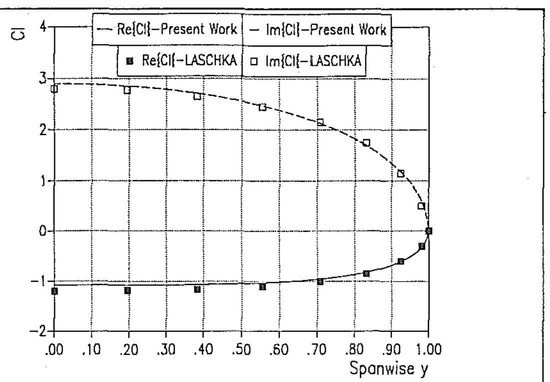

Fig. 4a. Sectional Lift Coefficient
Case : Fully Attached Flow, Heaving motion
M = 0.0, Xc = 0.25, k = 1.0, AR = 2

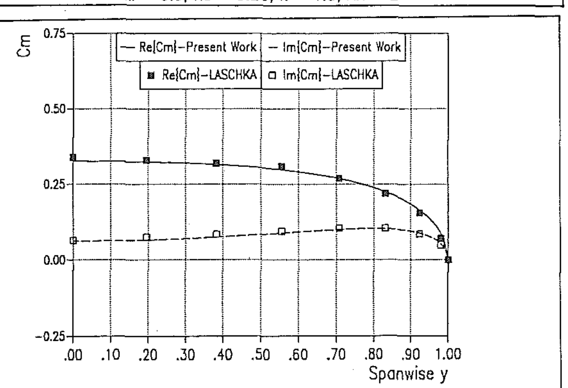

Fig. 4b. Sectional Moment Coefficient
Case : Fully Attached Flow, Heaving motion
M = 0.0, Xc = 0.25, k = 1.0, AR = 2

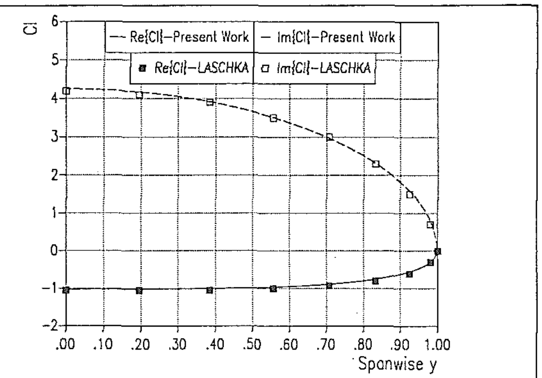

Fig. 5a. Sectional Lift Coefficient
Case : Fully Attached Flow, Heaving motion
M = 0.8, Xc = 0.25, k = 1.0, AR = 2

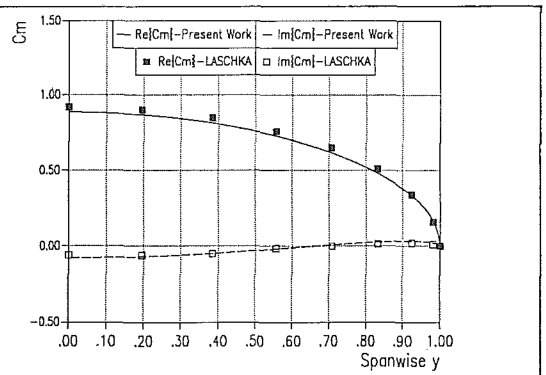

Fig. 5b. Sectional Moment Coefficient
Case : Fully Attached Flow, Heaving motion
M = 0.8, Xc = 0.25, k = 1.0, AR = 2

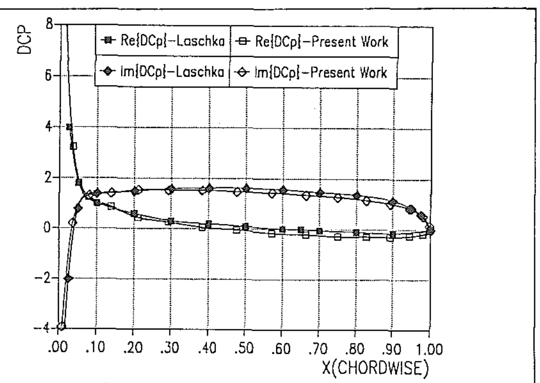

Fig. 6a. Delta CP at Section y = 0.9808
Case : Fully Attached Flow, Pitching Motion
M=0.0, k=2.0, AR=2, Xc = 0.5

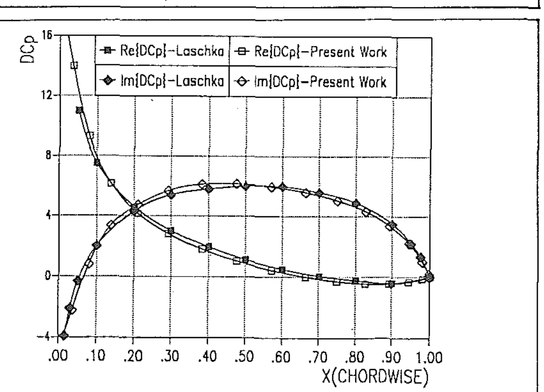

Fig. 6b. Delta CP at Section y = 0.0
Case : Fully Attached Flow, Pitching Motion
M=0.0, k=2.0, AR=2,Xc = 0.5

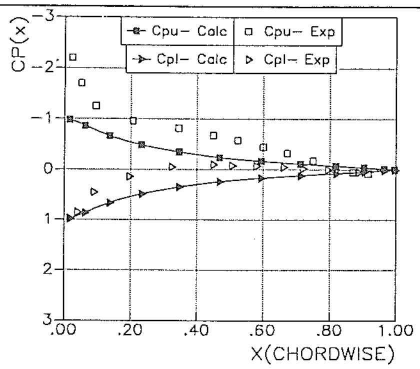

Fig. 7a. Qualitative Comparison for a Steady Result and Attached Flow situation
M=0.147, AR=4.444, y=0.2875, Exp NACA 64A2015

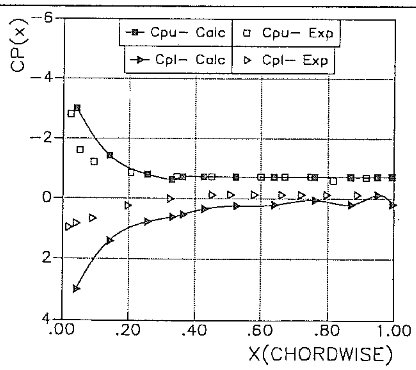

Fig. 7b. Qualitative Comparison for Steady Result and Partially Separated Flow situation
Xs=0.35, M=0.147, AR=4.444, y=0.2875, Exp. NACA 64A2015

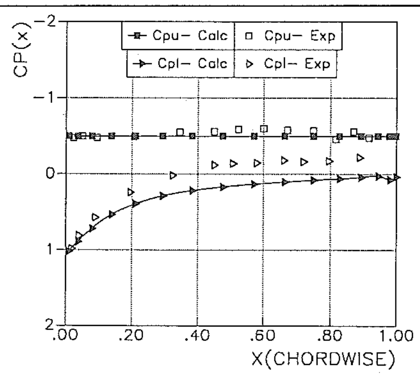

Fig. 7c. Qualitative Comparison for Steady Result and Fully Separated Flow situation
M=0.147, AR=4.444, y=0.2875, Exp NACA 64A2015

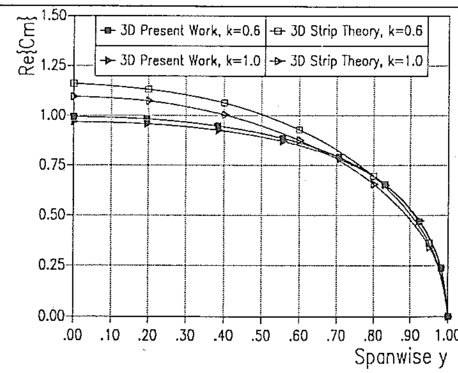

Fig. 8a. Influence of reduced frequency on Real part of Sectional Moment Coefficient
Case : Partially Separated Flow, Pitching Motion
Xs=0.6, M=0.0, Xc=0.5, AR=2, Gamma=0.0

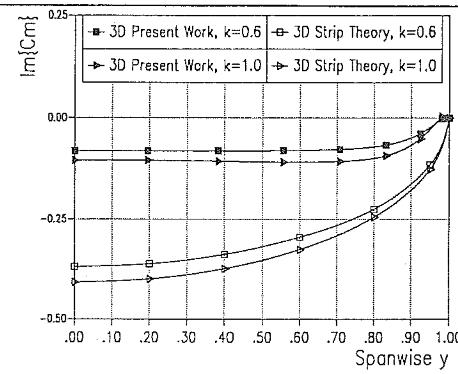

Fig. 8b. Influence of reduced frequency on Imaginary part of Sectional Moment Coefficient
Case : Partially Separated Flow, Pitching Motion
Xs=0.6, M=0.0, Xc=0.5, AR=2, Gamma=0.0

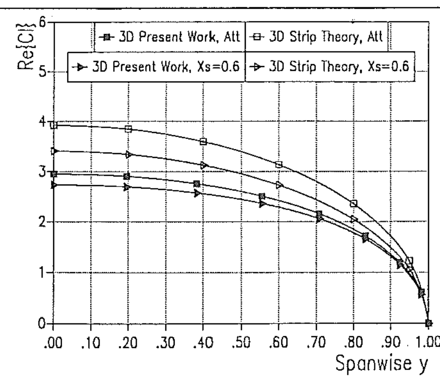

Fig. 9a. Real part of Sectional Lift Coefficient
Comparison of Separated and Attached Flow
Pitching Motion, M=0.0, Xc=0.5, k=1.0, AR=2, Gamma=0.0

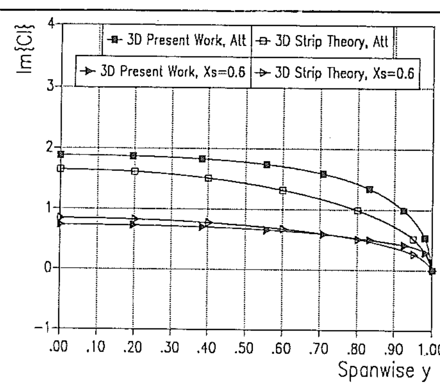

Fig. 9b. Imaginary part of Sectional Lift Coefficient
Comparison of Separated and Attached Flow
Pitching Motion, M=0.0, Xc=0.5, k=1.0, AR=2, Gamma=0.0